A Four-Layer DOI Detector With a Relative Offset for Use in an Animal PET System

Mikiko Ito, Jae Sung Lee, Sun Il Kwon, Geon Song Lee, Byungsik Hong, Kyong Sei Lee, Kwang-Souk Sim, Seok Jae Lee, June Tak Rhee, and Seong Jong Hong

***Abstract*—For animal PET systems to achieve high sensitivity without adversely affecting spatial resolution, they must have the ability to measure depth-of-interaction (DOI). In this paper, we propose a novel four-layer PET system, and present the performances of modules built to verify the concept of the system. Each layer in the four-layer PET system has a relative offset of half a crystal pitch from other layers. Performances of the four-layer detector were estimated using a GATE Monte Carlo simulation code. The proposed system consists of six H9500 PMTs, each of which contains 3193 crystals. A sensitivity of 11.8% was obtained at the FOV center position of the proposed system. To verify the concept, we tested a PET module constructed using a H9500 flat panel PMT and LYSO crystals of cross-sectional area 1.5×1.5 mm^2. The PET module was irradiated with a 1.8 MBq ^{22}Na radiation source from the front or side of the crystals to obtain flood images of each crystal. Collimation for side irradiation was achieved using a pair of lead blocks of dimension $50 \times 100 \times 200$ mm^3. All crystals in the four layers were clearly identified in flood images, thus verifying the DOI capability of the proposed four-layer PET system. We also investigated the optimal combination of crystal lengths in the four-layer PET system using the GATE Monte Carlo simulation code to generate events from simulated radiation sources, and using the ML-EM algorithm to reconstruct simulated radiation sources. The combination of short crystal lengths near radiation sources and long crystal lengths near the PMT provides better spatial resolution than combinations of same crystal lengths in the four-layer PET system.**

***Index Terms*—Depth of interaction (DOI)), four-layer animal PET, GATE Monte Carlo simulation, H9500 photomultiplier tube (PMT).**

Manuscript received September 25, 2009; revised December 11, 2009; accepted February 22, 2010. Date of current version June 16, 2010. This work was supported by the Korea Science and Engineering Foundation, Republic of Korea, under Grants M20709005465-07B0900-46510, M20709005465-08B0900-46510, and R01-2006-000-10296-0.

M. Ito is with the Department of Physics, Korea University, Seoul 126-701, Korea.

J. S. Lee is with the Departments of Nuclear Medicine, Biomedical Sciences and WCU Brain and Cognitive Sciences, Institute of Radiation Medicine, Medical Research Center, and Interdisciplinary Programs in Radiation Applied Life Science Major, Seoul National University, Seoul 110-744, Korea.

S. I. Kwon is with the Interdisciplinary Programs in Radiation Applied Life Science Major, Seoul National University College of Medicine, Seoul 110-744, Korea.

G. S. Lee is with the Department of Biomedical Engineering, Seoul National University College of Medicine, Seoul 110-744, Korea.

B. Hong, K. S. Lee, and K. S. Sim are with the Department of Physics, Korea University, Seoul 126-701, Korea.

S. J. Lee is with the Department of Biomedical Engineering, Seonam University, Namwon 590-911, Korea.

J. T. Rhee is with the Department of Physics, Konkuk University, Seoul 143-701, Korea.

S. J. Hong is with the Department of Radiological Science, Eulji University, Seongnam 461-731, Korea (e-mail: hongseongj@eulji.ac.kr).

Color versions of one or more of the figures in this paper are available online at http://ieeexplore.ieee.org.

Digital Object Identifier 10.1109/TNS.2010.2044892

I. Introduction

BECAUSE the imaging objects of animal PETs are small laboratory animals, the development of animal PET systems requires sensitivity and resolution improvements. For animal PET systems to achieve image qualities similar to those obtained using a human whole-body PET system, these systems must have a spatial resolution of less than 1 mm ($< 1\ \mu$l in volume) to match human PET systems with a spatial resolution of $\sim$ 10 mm ($\sim$ 1 ml). Furthermore, it is highly desirable that sensitivity be enhanced to collect enough a number of counts per image pixel, because the amount of radiopharmaceutical that can be injected into small laboratory animals is limited [1], [2]. Even though an animal PET system can be built with a small diameter increasing the coverage of solid angle, crystals with longer lengths are still needed to achieve high sensitivity.

On the other hand, the effect of parallax error, which affects the radial resolutions of off-center source distributions, is larger for animal PET systems with long crystals [2], [3]. Furthermore, the latest trend to use flat panel PMTs in animal PET systems result in a polygonal shape systems. In these systems, parallax errors affect spatial resolution even at the centers of the systems because gamma rays emitted from the center can enter crystals obliquely. However, the problems caused by the parallax error are eliminated if the DOI is known [4]. Consequently, a system capable of measuring DOI is required to improve sensitivity and spatial resolution.

Several detector structures that enable DOI measurements have been proposed. These are phoswich-type structures using several crystal materials with different decay times [5]–[7], an offset structure with a dual-layer has an offset of half a crystal pitch with each other [8], light sharing structures between layers using various reflector arrangements [9], [10], a structure constructed using crystals doped with different amounts of Ce [11], continuous DOI detectors composed of two detectors coupled to the opposite ends of single crystal array [12], [13], and a structure combining the phoswich-type with different crystals and an offset structure [14].

In the present study, we propose a novel offset structure for increasing sensitivity and resolution because it has several advantages. Since each crystal in the proposed design was surrounded by the ESR reflector, each crystal might be better separated in the flood map than the light sharing method proposed in [10]. We present test results of modules built to verify the DOI capability of the proposed four-layer PET system. The devised system has the advantages of simplicity using a same type of crystal DOI identification, and simpler readout electronics.

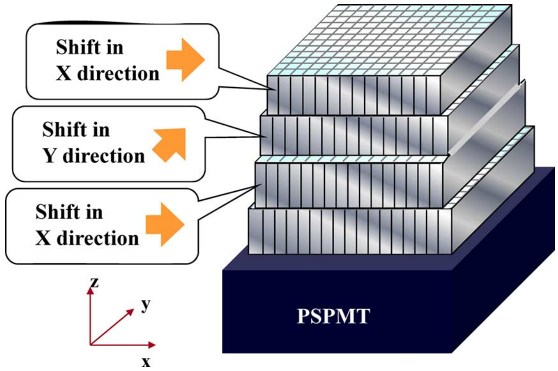

Fig. 1. A proposed four-layer PET module which shows the relative offset of each layer relative to the bottom layer.

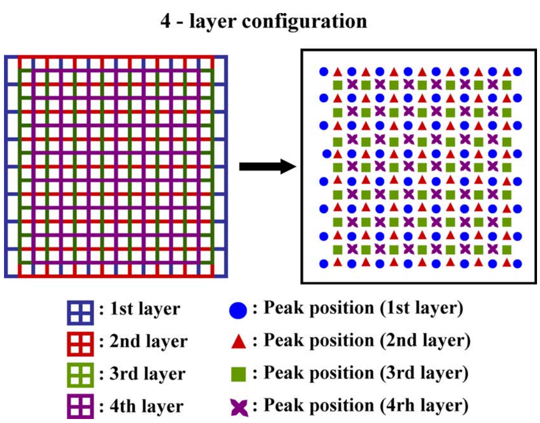

Fig. 2. Crystal arrangement of the proposed four-layer PET module and expected blobs in the flood map from each crystal layer.

II. Materials and Methods

A. Detector Configuration

We propose the novel structure shown in Fig. 1, in which all four crystal layers have a relative offset of half the crystal pitch with respect to each other. The crystals in each layer are off-set so that DOI information can be obtained using a 2-D (two-dimensional) position histogram. Crystal layers are shifted relative to the first layer. The shift distances are half the crystal pitch in the x-direction for the second layer, shift in both the x- and y-directions for the third, and in the y-direction only for the fourth. Fig. 2 shows an expected flood map, from which DOI information can be directly obtained.

B. GATE Simulation

A Monte Carlo simulation was used to investigate the performance of the four-layer PET system. We used a GATE simulation toolkit developed for the application of GEANT4 to medical imaging systems [15].

We considered a four-layer PET system consisted of six H9500 PMTs mounted with a crystal block of 3193 crystals. The system was hexagonal in shape, with the head-to-head distance of 84 mm between the two opposing detector modules. The crystal block was composed of four crystal layers, a 29×29 crystal array in the first layer, a 29×28 crystal array in the second layer, a 28×28 crystal array in the third layer, and a 28×27 crystal array in the fourth layer. Each crystal layer was offset as described above. The crystal layers consisted of LSO crystals of dimension $1.5 \times 1.5 \times 7\ \text{mm}^3$ with a crystal pitch of 1.565 mm.

To determine the efficiency of the system in the radial and axial directions, a ^{22}Na radiation source emitting two 511 keV annihilation gamma rays simultaneously in opposite directions was assumed to be positioned at various locations. The efficiency was calculated for energy window of $350 \sim 750$ keV.

To estimate the trans-axial and axial efficiencies and the spatial resolution of the system, following NEMA NU4-2008[16], the ^{22}Na point source was placed at the system center and at various radial offset positions. To normalize the geometric efficiency of each line of response, a F-18 planar source of dimension of 0.5 cm $\times$ 8.0 cm $\times$ 6.0 cm was also simulated [17]. Different effective planar source thicknesses were compensated for each line of response in normalization data. A DOI compression method that reduces computational cost while maintaining image quality was applied to the point source and normalization data [18]. A single-slice rebinning method was used to convert 3-D sinograms into 2-D sinograms [19]. For image reconstruction, an ML-EM algorithm was used with the pre-computed system matrix element, which was calculated as the area of intersection between each pixel and the rectangular line of response.

To determine radial and tangential resolutions at each position, profiles through count distribution peaks of point source were drawn in two orthogonal directions. Full width at half maximum (FWHM) values were then determined using a linear interpolation method [20], [21].

To investigate the optimal combination of crystal lengths, four-layer PET systems with four sets of different crystal lengths, i.e., (7.0 mm, 5.0 mm, 5.0 mm, 5.0 mm), (7.0 mm, 7.0 mm, 5.0 mm, 5.0 mm), and (7.0 mm, 7.0 mm, 7.0 mm, 7.0 mm), and (6.0 mm, 6.0 mm, 6.0 mm, 6.0 mm), where the first numbers correspond to the lengths of crystals close to the PMTs, were studied. The four sets of crystal length were selected to deduce the results of similar combinations using the results from the four sets. Two sets of crystal length, 7.0, 7.0, 5.0, 5.0 mm and 6.0, 6.0, 6.0, 6.0 mm, were selected to have the same total length with different arrangements of crystal length. The GATE Monte Carlo simulation code was used to generate events from simulated radiation sources positioned at the center and at off-center positions of 0.0 mm, 5.0 mm, 10.0 mm, 15.0 mm, 20.0 mm. The simulated radiation sources were reconstructed to estimate the spatial resolutions for the four sets of crystal lengths.

C. Testing of DOI Identification Using a Hamamatsu H9500 PMT

Since the proposed animal PET scanner employs four crystal layers, it is particularly suitable for a small animal PET scanner with high resolution and sensitivity. To determine the possibility of using crystals with a small cross-sectional area, we built two crystal blocks using LYSO crystals of dimension

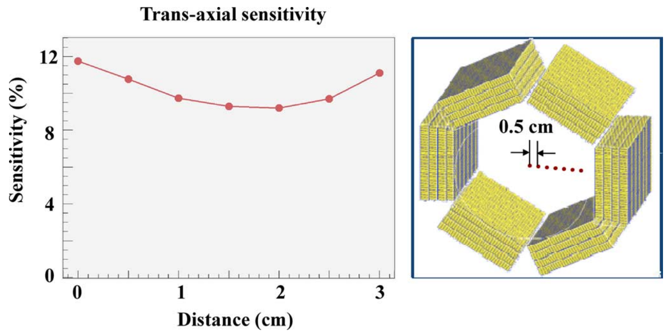

Fig. 3. Transaxial sensitivity as a function of trans-axial distance from the center.

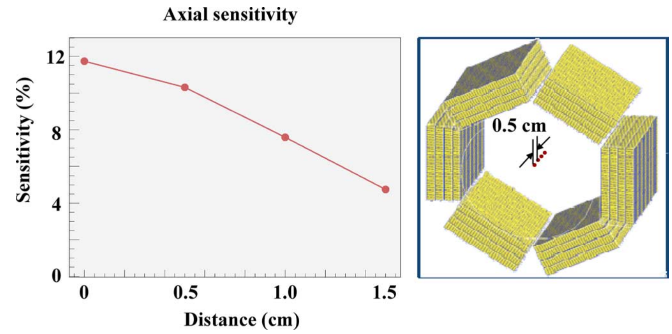

Fig. 4. Radial sensitivity as a function of radial distance from the center.

$1.5 \times 1.5 \times 7.0$ mm^3: a 7×7 crystal block in the first layer, a 6×7 crystal block in the second layer, a 6×6 crystal block in third layer, and a 5×6 crystal block in fourth layer. Accurate crystals arrangement in the offset configuration was required to separate peaks without overlapping in flood image. It was also important to have a minimal gap between crystals to minimize light loss between crystals. We constructed a matrix frame with crossing grids of 3M ESRs and inserted each crystal into the matrix frame [13]. The crystal block was optically coupled to a 256-channel flat panel H9500 PMT with an effective area of 49×49 mm^2. The assembled block was positioned at the center of the H9500 PMT, and the 256 anodes of the PS-PMT were connected to a resistor chain called a charge-division circuit which produced 4 output signals [22].

In order to obtain a flood image from each layer in the four-layer configuration separately, gamma photons collimated by the two lead blocks were directed at the side of the crystal block. The coincidence signal was generated using the dynode output of the flat panel H9500 PMT. This dynode output signal was inverted to negative polarity and then sent to a discriminator. The threshold voltage of the discriminator was set high enough to select only events produced by 511 keV gamma rays from a 0.37 MBq ^{22}Na radiation source positioned 10 cm away from the face of the crystal block. We interpreted the four output signals using a CAEN QDC967 module and determined the positions struck by photons using the four signals with an Anger-type calculation to obtain a flood image.

We also obtained a flood image of all four layers by irradiating the crystal block with the ^{22}Na radiation source from the front of the crystal block. For the signal readout, coincidence of two opposing H9500 PMTs was required.

III. Results

A. Simulation Results

Figs. 3 and 4 represent estimated efficiencies as a function of distance from the FOV center of the proposed four-layer PET system in radial and axial directions, respectively. Monte Carlo events were obtained by changing the source position in 5 mm intervals from the FOV center to 30 mm in the radial direction and to 15 mm in the axial direction. We obtained an efficiency of 11.8% at the center of the system, $9.2 \sim 11.8\%$ efficiencies in the trans-axial direction, and $4.8 \sim 11.8\%$ efficiencies in the axial direction.

TABLE I
The Ratios of Accepted Events in Each Crystal

Crystal lengths (in mm)	1st layer	2nd layer	3rd layer	4th layer
(7.0, 5.0, 5.0, 5.0)	1	1.1	1.5	1.8
(7.0, 7.0, 5.0, 5.0)	1	1.6	1.7	2.0
(7.0, 7.0, 7.0, 7.0)	1	1.7	2.8	3.8
(6.0, 6.0, 6.0, 6.0)	1	1.5	2.4	2.9

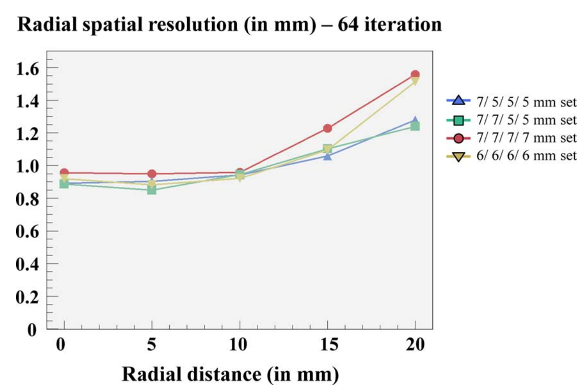

Fig. 5. Radial spatial resolution as a function of radial distance from the center.

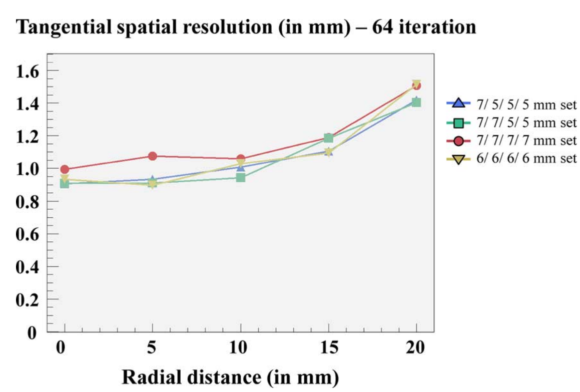

Fig. 6. Transaxial spatial resolution as a function of radial distance from the center.

Table I shows the ratios of accepted events of energy between 350 keV and 750 keV for the four sets of crystal lengths, i.e., (7.0 mm, 5.0 mm, 5.0 mm, 5.0 mm), (7.0 mm, 7.0 mm, 5.0 mm, 5.0 mm), (7.0 mm, 7.0 mm, 7.0 mm, 7.0 mm) and (6.0 mm, 6.0 mm, 6.0 mm, 6.0 mm), again where first numbers correspond to the lengths of crystals close to the PMT. Figs. 5 and 6 show radial and tangential spatial resolutions as a function of

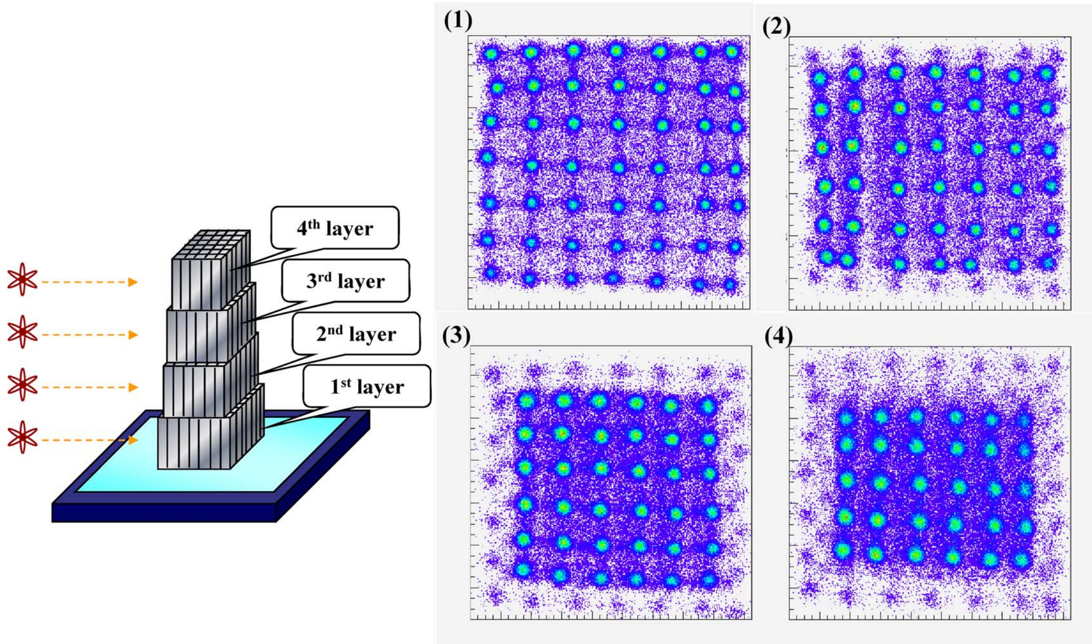

Fig. 7. Crystal arrangements and flood maps obtained with $1.5 \times 1.5 \times 7.0$ mm^3 crystals and Hamamatsu H9500 PMT. The crystals were side-irradiated with the ^{22}Na radiation source.

radial distances from the center of the scanner. The radial and tangential spatial resolutions were ~ 0.8 mm at the center of the scanner for all four sets of crystal lengths. As radial distance increased, radial and tangential spatial resolutions were relatively unchanged up to 10 mm even though they eventually became worse for radial distances greater than 10 mm. No differences in tangential spatial resolutions were observed for different sets of crystal lengths. The radial spatial resolution for the 7.0, 7.0, 7.0, 7.0 mm crystal set deteriorated more quickly than those of the 7.0, 5.0, 5.0, 5.0 mm and 7.0, 7.0, 5.0, 5.0 mm crystal sets. The radial and tangential spatial resolutions for the 7.0, 7.0, 5.0, 5.0 crystal set were better than those of the 6.0, 6.0, 6.0, 6.0 mm crystal set. As shown in Table I, the numbers of accepted events were more uniform for different crystal lengths than for same crystal lengths.

B. Experimental Results

Fig. 7 shows flood images, and horizontal and vertical projection histograms obtained using a H9500 PMT with coincidence detection when collimated gamma photons were irradiated into one layer of the four-layer configuration. The cross-sectional area of crystal was 1.5×1.5 mm^2. The number of peak positions in flood images was the same as the number of crystals in the irradiated layer.

Table II represents estimated FWHMs and mean values for the photoelectric peak of energy distribution of each layer in the four-layer configuration. The mean values of the photoelectric peak in the upper layer were smaller than those in the lower layer because scintillating photons were lost on the way to the PMT. Differences between first and fourth layer mean values were about 50%, indicating that the multiple energy window would be ideal for selecting photoelectric events. The energy resolution is 13.3% in the first, 17.7% in the second, 24.8% in the third, and 25.0% in the fourth layer. The timing resolution which was not measured is also expected to be worse in the fourth layer. As the distance between the surface of the flat panel PMT and the interaction position of gamma rays in crystal increased, the collection area of scintillation photons spread out, and scattering of optical photons increased because of the offset configuration.

TABLE II
MEAN ADC VALUES OF PHOTOELECTRIC PEAKS AND FWHM-TO-PITCH RATIOS OF BLOBS IN THE FLOOD MAP

	1^{st} layer	2^{nd} layer	3^{rd} layer	4^{th} layer
Mean ADC values of photoelectric peaks	4383	3257	2629	2190
FWHM-to-pitch ratios of blobs in the flood map	0.22	0.25	0.28	0.34

Fig. 8 shows a flood image of all four layers when gamma rays were irradiated at the front of the crystal block with coincident triggering using two H9500 PMTs. At the center of the flood image, peak positions were clearly separated from each other. On the other hand, image peak positions tended to overlap along the edge of the flood image, due to shifts in peak positions in the upper layer toward the center. These shifts were caused by a loss of photon collection along the edge of the crystal block.

IV. DISCUSSION

The proposed four-layer PET scanner has several advantages over existing DOI propositions. The most important one is the simplicity of the proposed scanner in that it uses only simple charge-division circuit boards and the same kind of crystals, while providing four-depth DOI capability. Each crystal layer stacked to form the four-layer crystal module can be built using

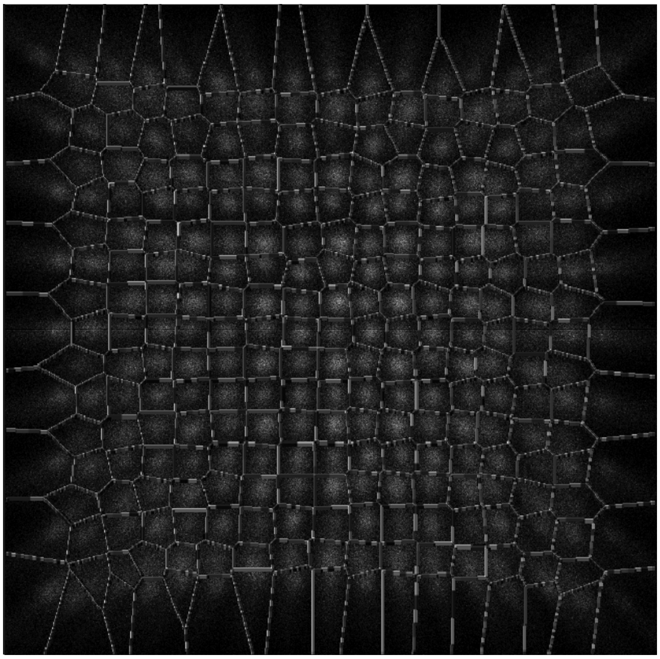

Fig. 8. Flood maps with $1.5 \times 1.5 \times 7.0$ mm^3 crystals and Hamamatsu H9500 PMT. The crystals were front-irradiated with the ^{22}Na radiation source.

the same method and the 3M ESR polymer grid. It is important that gaps between crystals are minimized to reduce light loss, this was achieved by using a matrix frame comprised of crossing grids of 3M ESR polymer of thickness 65 μm. However, we had to allow a 0.15 mm gap between crystals to accommodate variations in crystal sizes. In Table II, the mean ADC of the photoelectric photopeak in the crystal layer close to the PMT was larger by about 50% than the mean ADC close to the radiation source. This large difference forces discriminator thresholds to be set low enough so as not to lose events in the crystal layer close to the radiation source. We note that this difference is much larger than that of the four-layer configuration using a light-sharing technique, for which a difference of $\sim$20% was reported [23]. This ADC difference can be reduced by using a tighter gap between the crystals than the current gap (0.15 mm). Furthermore, although we focused on a small animal PET scanner with 6-PMT modules, the proposed PET scanner design could be easily expanded by increasing the number of PMT modules.

Because of the novel offset structure of the crystal layers, the distances between blobs in the flood map are half the crystal dimension if all blobs are projected into the same plane; this is equivalent to using half the crystal size to achieve better positional resolutions while reducing septal penetration due to a small crystal size. Since the projections of all blobs into the same plane is possible without losing DOI information when the DOI compression method [18] employed in this study is used, oversampling by a factor of two in the flood map would substantially improve the spatial resolutions of reconstructed images.

Since each PMT contains 3193 crystals in the proposed design, the pulse duration has to be limited to reduce the dead time. One of the possibilities is to use a small value of resistance in the charge division circuit to reduce the *RC* time constant.

Even though the four-layer PET scanner has radial and transaxial spatial resolutions of < 10 mm for radial distances of < 10 mm, image reconstruction can be complicated and time-consuming if the fully 3-D image reconstruction method without DOI compression is applied to obtain best spatial resolution. However, faster image reconstructions can be achieved by using parallel computation techniques (i.e., by using multiple graphical processor units in parallel).

V. Summary and Conclusion

We proposed a novel structure for a DOI detector in which all four crystal layers have an offset of a half the crystal pitch relative to each other. The performances of the proposed system with a four-layer configuration were estimated by GATE Monte Carlo simulation. A sensitivity of 11.8% was obtained at the center of the proposed configuration using this simulation method.

We acquired data using H9500, and obtained flood images for each layer and for all layers in the four-layer configuration. All the crystals were clearly identified at the center of the PMT, but the crystals around the PMT edge were less well separated in flood images. A modified charge-division circuit may help crystal separation around the edge [10].

In the present study, we show that the devised four-layer configuration with crystal layer offsets clearly identifies all crystals in flood images. We are confident that this relative offset concept could be used to produce an animal PET scanner with high spatial resolution and sensitivity.

References

[1] E. M. Jagoda, J. J. Vaquero, J. Seidel, M. V. Green, and W. C. Eckelman, "Experiment assessment of mass effects in the rat: Implications for small animal PET imaging," *Nucl. Med. Biol.*, vol. 31, pp. 771–779, 2004.

[2] M. G. Pomper and J. S. Lee, "Small animal imaging in drug development," *Curr. Pharm. Des.*, vol. 11, no. 25, pp. 3247–3272, 2005.

[3] E. J. Hoffman, T. M. Guerreo, G. Germano, W. M. Diqby, and M. Dahlbom, "PET system calibrations and corrections for quantitative and spatially accurate images," *IEEE Trans. Nucl. Sci.*, vol. 36, pp. 1108–1112, 1989.

[4] L. R. MacDonald and M. Dahlbom, "Parallax correction in PET using depth of interaction information," *IEEE Trans. Nucl. Sci.*, vol. 45, pp. 2232–2237, 1998.

[5] M. Dahlbom, L. R. MacDonald, L. Eriksson, M. Paulus, M. Andreaco, M. E. Casey, and C. Moyers, "Performance of a YSO/LSO phoswich detector for use in a PET/SPECT system," *IEEE Trans. Nucl. Sci.*, vol. 44, pp. 1114–1119, 1997.

[6] J. Seidel, J. J. Vequero, S. Sieqel, W. R. Gandler, and M. V. Green, "Depth identification accuracy of a three layer phoswich PET detector module," *IEEE Trans. Nucl. Sci.*, vol. 46, pp. 485–490, 1999.

[7] M. Streun, G. Brandenburg, H. Larue, H. Saleh, E. Zimmermann, K. Ziemons, and H. Halling, "Pulse shape discrimination of LSO and LuYAP scintillators for depth of interaction detection in PET," *IEEE Trans. Nucl. Sci.*, vol. 3, pp. 1636–1639, 2002.

[8] N. Zhang and C. J. Thompson, "Optimizing position readout circuits in positron emission tomography front-end electronics," *IEEE Trans. Nucl. Sci.*, vol. 50, pp. 1398–1403, 2003.

[9] H. Murayama, H. Ishibashi, H. Uchida, T. Omura, and T. Yamashita, "Depth encoding multicrystal detectors for PET," *IEEE Trans. Nucl. Sci.*, vol. 45, pp. 1152–1157, 1998.

[10] N. Inadama, H. Murayama, M. Watanabe, T. Omura, T. Yamashita, H. Kawai, T. Umehara, T. Kasahara, N. Orita, and T. Tsuda, "Performance of a PET detector with a 256 ch flat panel PS-PMT," *IEEE Trans. Nucl. Sci.*, vol. 51, pp. 58–62, 2004.

[11] S. Yamamoto and H. Ishibashi, "A GSO depth of interaction detector for PET," *IEEE Trans. Nucl. Sci.*, vol. 45, pp. 1078–1082, 1998.

[12] W. W. Moses, S. E. Derenzo, C. L. Melcher, and R. A. Manente, "A room temperature LSO/Pin photodiode PET detector module that measures depth of interaction," *IEEE Trans. Nucl. Sci.*, vol. 42, pp. 1085–1089, 1995.

[13] Y. Shao, R. W. Silverman, R. Farrell, L. Cirignano, R. Grazioso, K. S. Shah, G. Visser, M. Clajus, T. O. Tumer, and S. R. Cherry, "Design studies of a high resolution PET detector using APD arrays," *IEEE Trans. Nucl. Sci.*, vol. 47, pp. 1051–1057, 2000.

[14] S. J. Hong, S. I. Kwon, M. Ito, G. S. Lee, K.-S. Sim, K. S. Park, J. T. Rhee, and J. S. Lee, "Concept verification of three-Layer DOI detectors for small animal PET," *IEEE Trans. Nucl. Sci.*, vol. 55, pp. 912–917, 2008.

[15] S. Jan *et al.*, "GATE: A simulation toolkit for PET and SPECT," *Phys. Med. Biol.*, vol. 49, pp. 4543–4561, 2004.

[16] "Performance Measurements for Small Animal Positron Emission Tomographs (PETs)," NEMA Standards, Rosslyn, VA, Publication NU 4-2008, 2008.

[17] E. J. Hoffman, T. M. Guerrero, G. Germano, W. M. Digby, and M. Dahlbom, "PET system calibrations and corrections for quantitative and spatially accurate images," *IEEE Trans. Nucl. Sci.*, vol. 36, pp. 1108–1112, 1989.

[18] T. Yamaya, N. Hagiwara, T. Obi, M. Yamaguchi, K. Kita, N. Ohyama, K. Kitamura, T. Hasegawa, H. Haneishi, and H. Murayama, "DOI-PET image reconstruction with accurate system modeling that reduces redundancy of the imaging system," *IEEE Trans. Nucl. Sci.*, vol. 50, pp. 1404–1409, 2003.

[19] M. E. Daube-Witherspoon and G. Muehllehner, "Treatment of axial data in three-dimensional PET," *J. Nucl. Med.*, vol. 28, pp. 1717–1724, 1987.

[20] M. E. Daube-Witherspoon, J. S. Karp, M. E. Casey, F. P. Difilippo, H. Hines, G. Muehllehner, V. Simcic, C. W. Stearns, L.-E. Adam, S. Kohlmyer, and V. Sossi, "PET performance measurements using the NEMA NU 2-2001 standard," *J. Nucl. Med.*, vol. 43, pp. 1398–1409, 2002.

[21] J. S. Kim, J. S. Lee, K. C. Im, S. J. Kim, S. Y. Kim, D. S. Lee, and D. H. Moon, "Performance measurement of the microPET focus 120 scanner," *J. Nucl. Med.*, vol. 48, pp. 1527–1535, 2007.

[22] S. I. Kwon, S. J. Hong, M. Ito, H. S. Yoon, G. S. Lee, K. S. Sim, J. T. Rhee, D. S. Lee, and J. S. Lee, "Development of position encoding circuit for a multi-anode position sensitive photomultiplier tube," *Nucl. Med. Mol. Imag.*, vol. 42, pp. 469–477, 2008.

[23] N. Inadama, H. Murayama, T. Yamaya, K. Kitamura, T. Yamashita, H. Kawai, T. Tsuda, M. Sato, Y. Ono, and M. Hamamoto, "Preliminary evaluation of four-layer BGO DOI-detector for PET," *IEEE Trans. Nucl. Sci.*, vol. 53, pp. 30–34, 2006.